

## THE A<sup>V</sup>-B<sup>VI</sup>-I TERNARY SYSTEMS: A BRIEF REVIEW ON THE PHASE EQUILIBRIA REVIEW

© 2019 Z. S. Aliev<sup>✉</sup>

*Azerbaijan State Oil and Industry University  
20, Azadlig ave., AZ1010 Baku, Azerbaijan*

**Abstract.** This paper presents a brief review on the ternary phase equilibria in the ternary A<sup>V</sup>-B<sup>VI</sup>-I systems (A<sup>V</sup> = Sb, Bi; B<sup>VI</sup> = S, Se, Te). These systems includes the series of ternary compounds those are very attractive source materials for photo-, thermos- and ferroelectric energy transformation along the recently discovered semiconductors that exhibit Rashba-type spin splitting in their surface states. In the Rashba semiconductors, a unique toroidal 3D Fermi surface appears on the crystal surface, which leads to unusual properties that make it possible to realize unique electronic devices based on these compounds. The thorough knowledge on the ternary phase diagram of these systems shed light on the chemical and structural design of new multifunctional materials with tunable properties. This knowledge is very important when focusing on the chemistry of such multifunctional materials based on complex element systems.

**Keywords:** phase diagram; phase equilibria; antimony sulfoiodide; bismuth selenoiodide; bismuth telluroiodide.

### 1. INTRODUCTION

Sulfo-, seleno- and tellurohalides of a group 15 metals have been intensively investigated over the last four decades as photo-, thermo- and ferroelectric materials [1–5]. During last four decades, there is an increasing interest for A<sup>V</sup>B<sup>VI</sup>C<sup>VII</sup>-type ternary compounds due to their intriguing electronic properties, both in the single crystal form and thin film [6]. For example, SbSI was one of the most studied member of this family and so far, there is much information on its physical properties [7–12]. It has potential in applications ranging from optical light modulators, electroacousto-optical transformers, piezoelements to sensitive low-pressure gauges etc. On the other hand, since the giant Rashba-type spin splitting has recently been reported in the polar-layered non-centrosymmetric BiTeI [13–14], the bismuth containing tellurohalides became one of the much more attractive materials in the condensed matter physics [15–18]. These materials exhibit a strong spin-orbit interaction effect that opens a new pathway for the realization of spin-based electronic devices based on them.

✉ Aliev Ziya S., e-mail: ziyasaliev@gmail.com,  
ziya.aliev@asoiu.edu.az



Контент доступен под лицензией Creative Commons Attribution 4.0 License.  
The content is available under Creative Commons Attribution 4.0 License.

Rational design and development of such ternary or quaternary new phases and solid solutions with a non-centrosymmetric crystal structure, as well as with a variable chemical composition, is of considerable interest for optimizing properties. Given the growing interest in this class of materials, a thorough study of phase diagrams for the respective element systems is of particular importance in the search for proper baseline compositions in order to develop materials with optimized properties [19–20]. Here, we focus on the reviewing of the ternary phase equilibria in the A<sup>V</sup>-B<sup>VI</sup>-I systems. This review can shed light on the chemical design of the new phases with variable compositions based on the starting multifunctional compounds of the systems, like SbSI, SbTeI, BiSI, BiSeI, BiTeI, etc.

### 2. PHASE DIAGRAMS OF THE A<sup>V</sup>-B<sup>VI</sup>-I SYSTEMS

#### 2.1. The Sb-S-I system

As mentioned above, the Sb-S-I system has attracted much more attention thanks to its ternary compound SbSI which is most studied member of the family of A<sup>V</sup>B<sup>VI</sup>C<sup>VII</sup>-type ternary compounds [1, 2, 7–12, 21]. Until our through investigation on this

system, the binary  $\text{SbI}_3$ – $\text{Sb}_2\text{S}_3$  section was only studied in this system. Two different literature reports exist on the phase diagram of this section [22, 23]. Belyayev [22] reported that this section includes the only compound  $\text{SbSI}$ , which melts congruently at 650 K. The eutectic composition between  $\text{SbSI}$  and  $\text{Sb}_2\text{S}_3$  has the melting point of 595 K at about 75 mol %  $\text{Sb}_2\text{S}_3$ , whereas the eutectic between  $\text{SbSI}$  and  $\text{Sb}_2\text{S}_3$  is degenerated close to  $\text{SbI}_3$  at 443 K. Ryzantsev and co-authors [23] reported slightly different data on the melting point of  $\text{SbSI}$  and eutectic compositions.  $\text{SbSI}$  melts congruently at 675 K according to this work and has a narrow homogeneity region. Our DTA, XRD data and the results of the microhardness for the selected compositions [24] (Fig. 1) agree well with the data of Ref. [23]. The congruent melting temperature of  $\text{SbSI}$  was determined to be 675 K which agrees well with reported data [23] whereas 25 °C higher than data of [22]. The main discrepancy is related to the form of the liquidus curve of  $\text{SbSI}$ . According to our data, the liquidus surface of  $\text{SbSI}$  has a *S*-shape form, which is typical for the systems that have a tendency for immiscibility, however, it represented as convex curve in Ref. [23] typical for dystectic type equilibrium. The crystal structure of  $\text{SbSI}$  is reported in the literature [25, 26]. Three phases of this compound have been reported: ferroelectric ( $T < 295$  K), antiferroelectric ( $295 \text{ K} < T < 410$  K) and paraelectric ( $T < 410$  K) [1]. Both in the paraelectric and ferroelectric phase, it crystallizes in the orthorhombic structure with space group  $Pnam$  ( $a = 8.556(3)$  Å;  $b = 10.186(4)$  Å;  $c = 4.111(2)$  Å;  $z = 4$ ) and  $Pna2_1$  ( $a = 8.53$  Å;  $b = 10.14$  Å;  $c = 4.10$  Å), according to [25] and [26], respectively. As can be seen from the global phase diagram of the system, (Fig. 2) [24], the primary crystallization field of the  $\text{SbSI}$  is quite large and occupies considerable part of the total area of the composition triangle, which provides a variety of compositions of the melts for growing single crystals of the  $\text{SbSI}$ . However, the largest primary crystallization field belongs to elemental antimony. Two wide immiscibility fields were detected in this system. The first one ( $L_1 + L_2$ ) starts from the  $\text{Sb}$ – $\text{I}$  system ( $m_3 m_3'$ ) and joins to immiscibility field of the  $\text{Sb}$ – $\text{Sb}_2\text{S}_3$  subsystem ( $m_1 m_1'$ ) over the  $\text{Sb}$ – $\text{SbSI}$  section ( $m_4 m_4'$ ). It almost covers the primary crystallization field of antimony in the  $\text{Sb}$ – $\text{SbI}_3$ – $\text{Sb}_2\text{S}_3$  subsystem. The primary crystallization field of elemental sulfur and some in- and monovariant equilibria are degenerated and is positioned very close to the elemental sulfur corner of the composition triangle. A schematic description of this area is given in Fig. 2 as a blow-up inset.

## 2.2. The Sb–Se–I system

The literature review shows that the ternary  $\text{Sb}$ – $\text{Se}$ – $\text{I}$  system was investigated so far along the various isopleth sections. However, among them the quasi-binary  $\text{Sb}_2\text{Se}_3$ – $\text{SbI}_3$  section was the most studied one [27, 28–32]. According to Ref. [28] this section hosts the only compound  $\text{SbSeI}$  that melts congruently at 721 K, whereas the eutectic compositions were found to be 69 and 3 mol %  $\text{Sb}_2\text{S}_3$  at temperatures 703 and 428 K, respectively. Other authors [29, 30] report slightly different data on the melting points and eutectic compositions. The thermal analysis results in our previous investigation [27] for the selected alloys in this system showed the well coincidence with the data reported by Dolgikh and co-authors [29]. The congruent melting character of the  $\text{SbSeI}$  at 725 K is confirmed. Its eutectic mixture with the  $\text{Sb}_2\text{Se}_3$  crystallizes at 58 mol %  $\text{Sb}_2\text{S}_3$  at 716 K whereas, the eutectic with  $\text{SbI}_3$  is almost degenerated (Fig. 3) [27]. The  $\text{SbI}_3$ – $\text{Se}$  and  $\text{SbSeI}$ – $\text{Se}$  quasi-binary sections are shown to be of eutectic type. The eutectic compositions have melting point of 433 and 428, respectively, and have 62 and 74 mol %  $\text{Se}$  [31].  $\text{SbSeI}$  crystallizes in the  $\text{SbSI}$  structure type, space group  $Pnma$ , with the unit cell parameters  $a = 8.6862(9)$ ,  $b = 10.3927(9)$ ,  $c = 4.1452(3)$  Å [4]. The self-consistent phase diagram of the  $\text{Sb}$ – $\text{Se}$ – $\text{I}$  system [27] (Fig. 4) was plotted by us at first time. It consists of six fields corresponding to primary crystallization of the elemental components

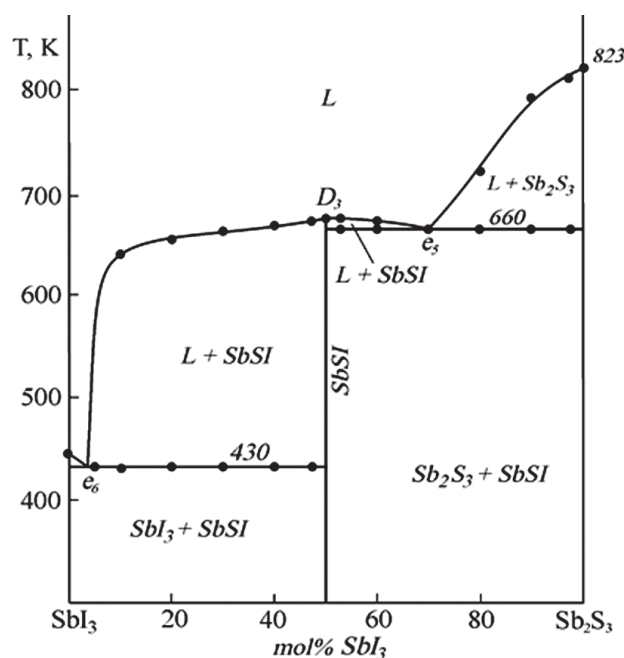
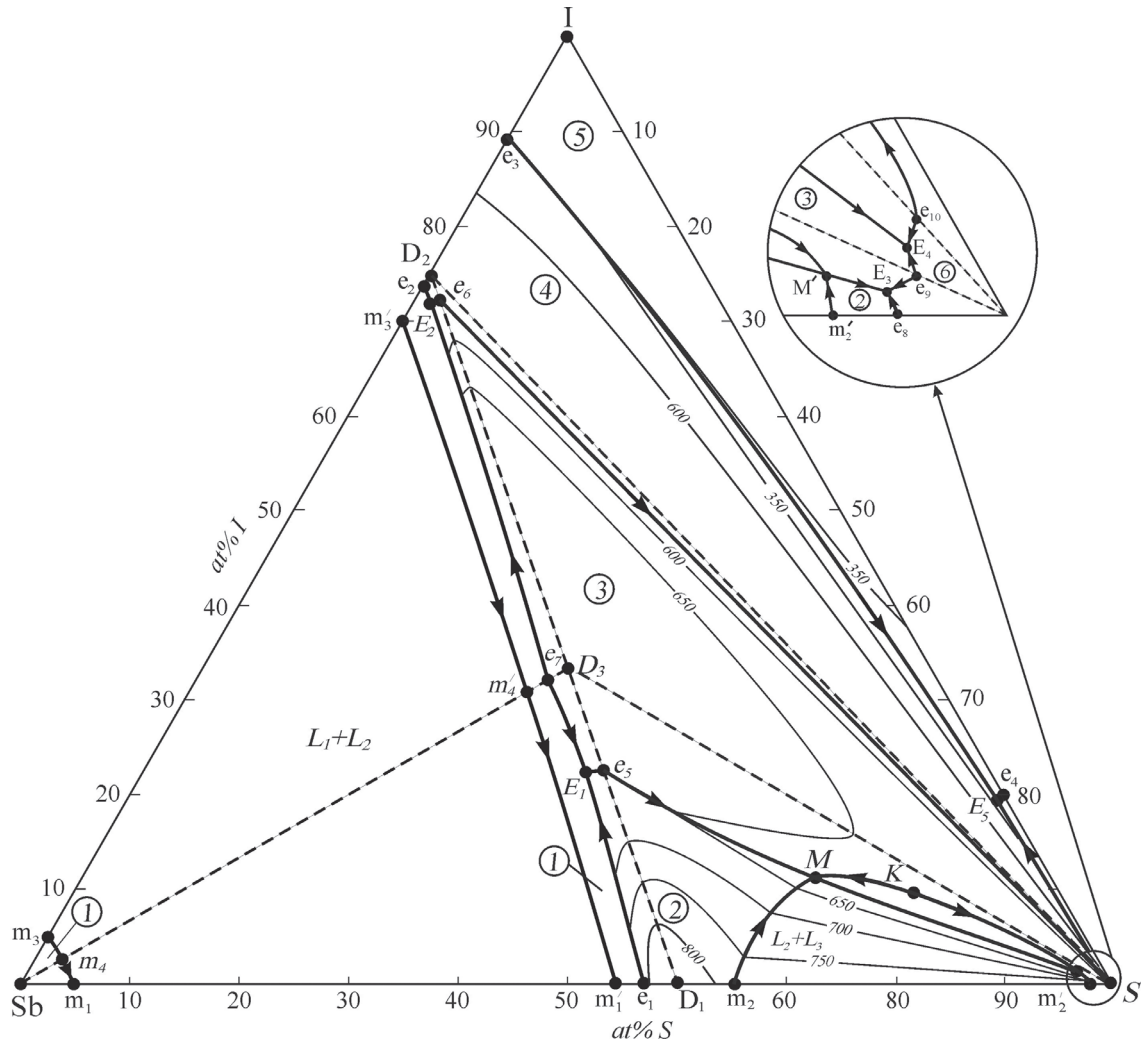
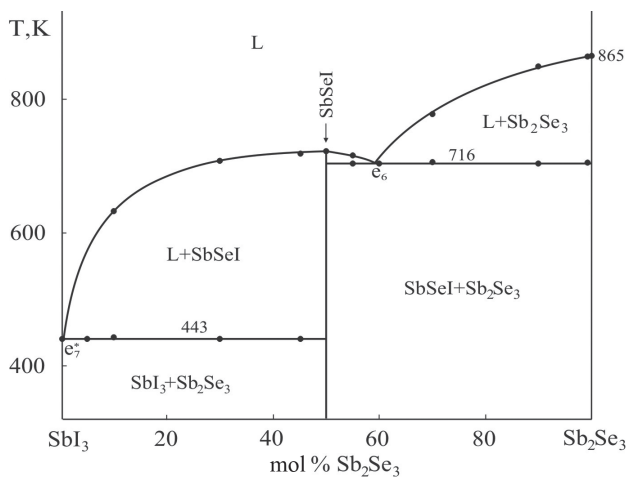


Fig. 1. Phase diagram of the  $\text{SbI}_3$ – $\text{Sb}_2\text{S}_3$  quasi-binary system [23, 24]



**Fig. 2.** The phase diagram of the Sb-S-I system [24]. Primary crystallization fields of the phases: 1 - Sb; 2 -  $Sb_2S_3$ ; 3 - SbSI; 4 -  $SbI_3$ ; 5 -  $I_2$ ; 6 - S



**Fig. 3.** Phase diagram of the  $SbI_3-Sb_2Se_3$  system [29]. Black dots show our data [27]

and compounds  $Sb_2Se_3$ ,  $SbI_3$  and  $SbSeI$ . Similar to Sb-S-I system, it also exhibits the broad immiscibility region ( $m_1m_3m_2m'_2m'_3m'_1$ ), which lies within the field of primary crystallization of antimony and overlaps with 90 % of its area. The quasi-binary sections (dashed lines in Fig. 4) triangulate the Sb-Se-I system forming five independent subsystems. They are Sb- $Sb_2Se_3$ -SbSeI, Sb- $SbI_3$ -SbSeI, SbSeI- $SbI_3$ -Se,  $Sb_2Se_3$ -SbSeI-Se, and  $SbI_3$ -Se- $I_2$ . The two former subsystems are characterized by monotectic and eutectic equilibria whereas; the other subsystems belong to the ternary eutectic type.

### 2.3. The Sb-Te-I system

The literature data on the phase equilibria of Sb-Te-I system contained several reports on various isopleth sections [32, 33-37], among which the quasibinary  $Sb_2Te_3-SbI_3$  section was the most stu-

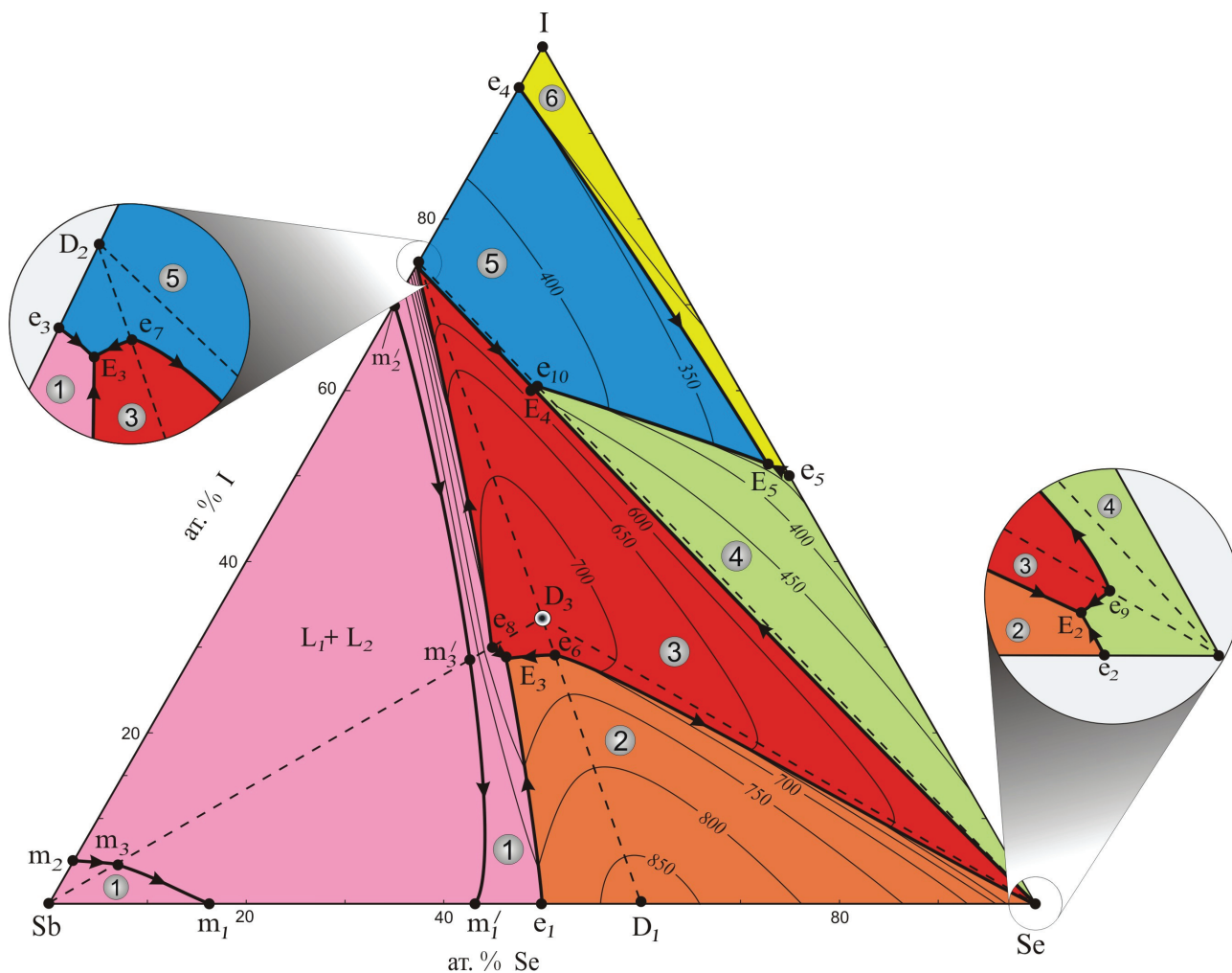


**Fig. 4.** The phase diagram of the Sb–Se–I system [27]. Primary crystallization fields are: 1 – Sb; 2 –  $\text{Sb}_2\text{Se}_3$ ; 3 – SbSeI; 4 – Se; 5 –  $\text{SbI}_3$ ; 6 –  $\text{I}_2$

died [8–12]. Belotskiy shown [33, 34] that the section  $\text{Sb}_2\text{Te}_3$ – $\text{SbI}_3$  contains the only compound SbTeI, which melts congruently at 633 K. Other authors [35–37] report results that are different from those of Belotskiy's data [33, 34]. These works show that the ternary compound SbTeI melts incongruently by a peritectic reaction at 643 [35, 36] or 675 K [37]. Our DTA data and the results of the microhardness and EMF measurements for the selected compositions confirm the data of [35, 36], (Fig. 5).

SbTeI is the only ternary compound in the Sb–Te–I system. It crystallizes in the monoclinic space group  $C2/m$  with the unit cell parameters  $a = 13.701$ ,  $b = 4.2418$ ,  $c = 9.201$  Å [38]. Its crystal structure represents a unique monoclinic variation of the SbSI structure type [39], in which typical for these structures (SbTe) double chains run along the  $b$  axis and alternate with the iodine atoms in the  $ac$  plane. Such a monoclinic distortion of the SbSI type is stable and persists even when 90 % of the antimony is re-

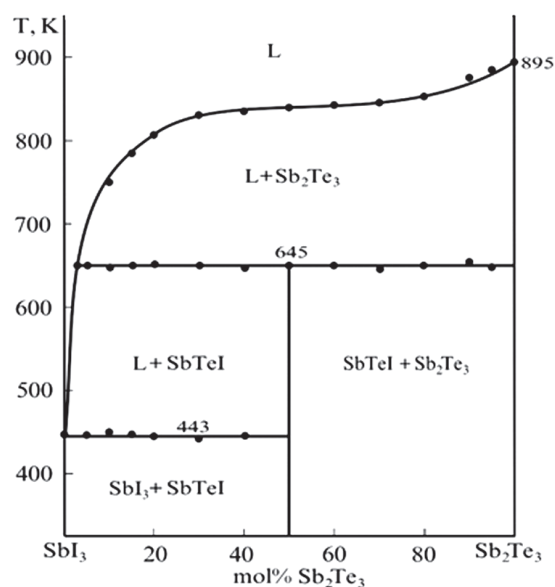


**Fig. 5.** Phase diagram of the  $\text{SbI}_3$ – $\text{Sb}_2\text{Te}_3$  system [35, 36]. Black dots shows our data [32]

placed by bismuth and transforms into the trigonal BiTeI structure only with greater bismuth concentration [40, 41]. The complete phase diagram of the ternary Sb–Te–I system has been investigated by us in [32]. The system (Fig. 6) have a quite complex phase relationships [32]. One can see that the area of the primary crystallization of SbTeI is degenerate near  $SbI_3$  indicate that grows of its large single crystal from melt is a difficult process. The system Sb–Te–I is divided by three quasi-binary sections in the following four independent subsystems:  $SbI_3$ – $TeI_4$ – $I_2$  (A),  $SbI_3$ – $TeI_4$ –Te (B),  $SbI_3$ –Te– $Sb_2Te_5$  (C) and  $Sb$ – $SbI_3$ – $Sb_2Te_5$  (D). The subsystem (A) relates to the invariant eutectic type, whereas the wide immiscibility region was found in the subsystem (B). The subsystem (C) is characterized by eutectic and monotectic reactions, whereas the existence of the eutectic, monotectic and transition reactions and a wide immiscibility region characterize the subsystem (D).

#### 2.4. The Bi–S–I system

The complete phase diagram of the Bi–S–I ternary system has been reported in our paper [42] at first time. Nevertheless, up to this report only

the quasi-binary  $BiI_3$ – $Bi_2S_3$  system was studied by Ryazantsev et al. [43]. According to this work, it is a quasi-binary one and includes two ternary compounds, namely BiSI and  $Bi_{19}S_{27}I_3$ . These compounds melt peritectically at 808 and 990 K, respectively. The compositions of the peritectic points along the section lie at 35 and 80 mol %  $Bi_2S_3$ , respectively. The eutectic reaction was found to occur at 668 K and 4 mol %  $Bi_2S_3$ . The thermodynamic properties of the both ternary compounds in this system were obtained by Oppermann and Petasch [44]. Our DTA and XRD results for the selected compositions agree well with the result of [43] (Fig. 7). The detailed investigations confirm the existence both of ternary compounds BiSI and  $Bi_{19}S_{27}I_3$ . The crystal structures of both compounds are well studied. BiSI crystallizes in the orthorhombic space group  $Pnma$  with the lattice parameters  $a = 8.529$ ,  $b = 4.172$ ,  $c = 10.177$  Å and  $z = 4$  [45].  $Bi_{19}S_{27}I_3$  has a hexagonal lattice, space group  $P63/m$ , with  $a = 15.640$ ,  $c = 4.029(2)$  Å, and  $z = 2/3$ . BiSI crystallizes in the BiSBr structure type (also referred to as the SbSBr type) and features one-dimensional BiSI strands with the considerably elongated Bi–I distance of 3.0 Å that run along

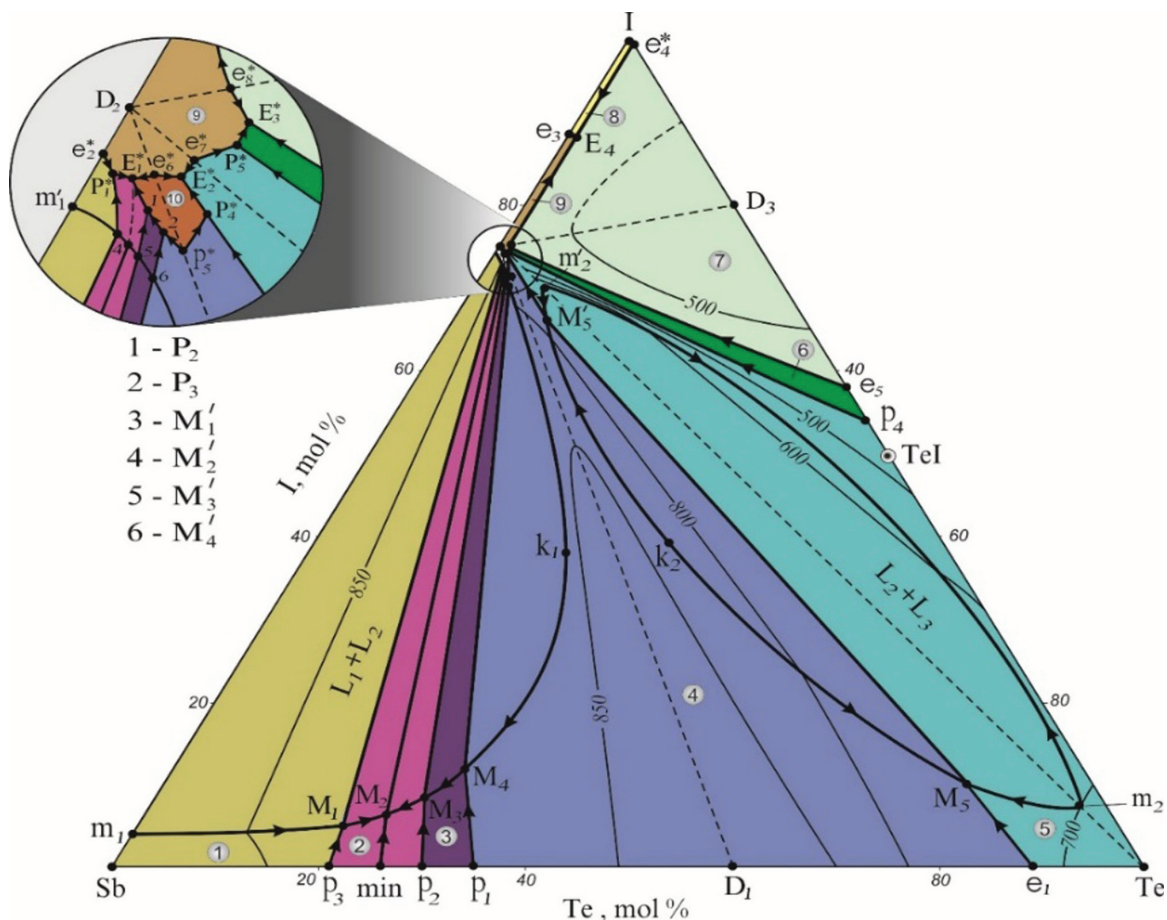


**Fig. 6.** The phase diagram of the Sb–Te–I system [32]. Primary crystallization areas of phases: 1 –  $\alpha$ ; 2 –  $\delta$ ; 3 –  $\gamma$ ; 4 –  $Sb_2Te_5$ ; 5 – Te; 6 – TeI; 7 –  $TeI_4$ ; 8 –  $I_2$ ; 9 –  $SbI_3$ ; 10 – SbTeI

the *c* axis. The slabs are joined into a 3D structure through non-covalent Bi–I interactions at 3.7 Å. In the crystal structure of  $\text{Bi}_{19}\text{S}_{27}\text{I}_3$ , the slabs running along the *c* axis are formed only by bismuth and sulfur atoms; they are further connected through disordered Bi(1) atoms, whereas the iodine atoms sit in the voids, with the Bi–I distances exceeding 3.5 Å. Taking into account the details of the crystal structure of  $\text{Bi}_{19}\text{S}_{27}\text{I}_3$ , it is frequently formulated as  $\text{Bi}(\text{Bi}_2\text{S}_3)_9\text{I}_3$  [45]. The phase diagram of the system (Fig. 8) [42] shows the existence of the ten primary crystallization fields. The primary crystallization fields of the binary  $\text{BiI}_3$ ,  $\text{Bi}_2\text{S}_3$  and ternary  $\text{Bi}_{19}\text{S}_{27}\text{I}_3$ ,  $\text{BiSI}$  compounds are found to be very large and occupy major part of the total area of the Bi–S–I triangle. Two wide immiscibility fields are observed in this system. The first one ( $L_1 + L_2$ ) starts from the Bi–I system ( $m_2m_2'$ ) and spreads into the Bi– $\text{BiI}_3$ – $\text{Bi}_2\text{S}_3$

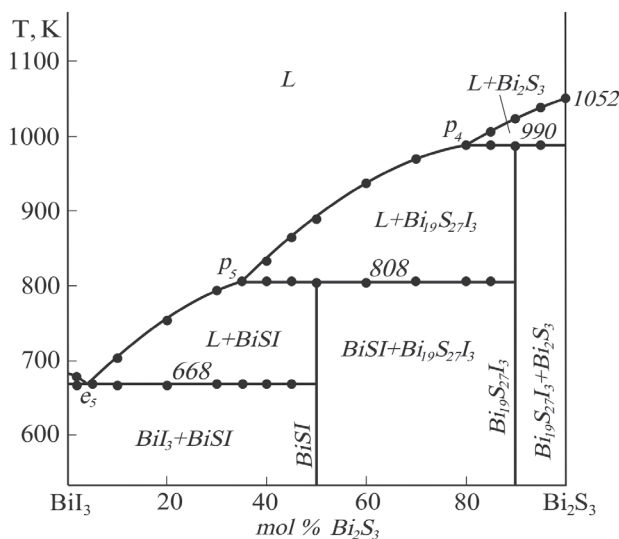


Fig. 7. Phase diagram of the  $\text{BiI}_3$ – $\text{Bi}_2\text{S}_3$  system [43, 44]

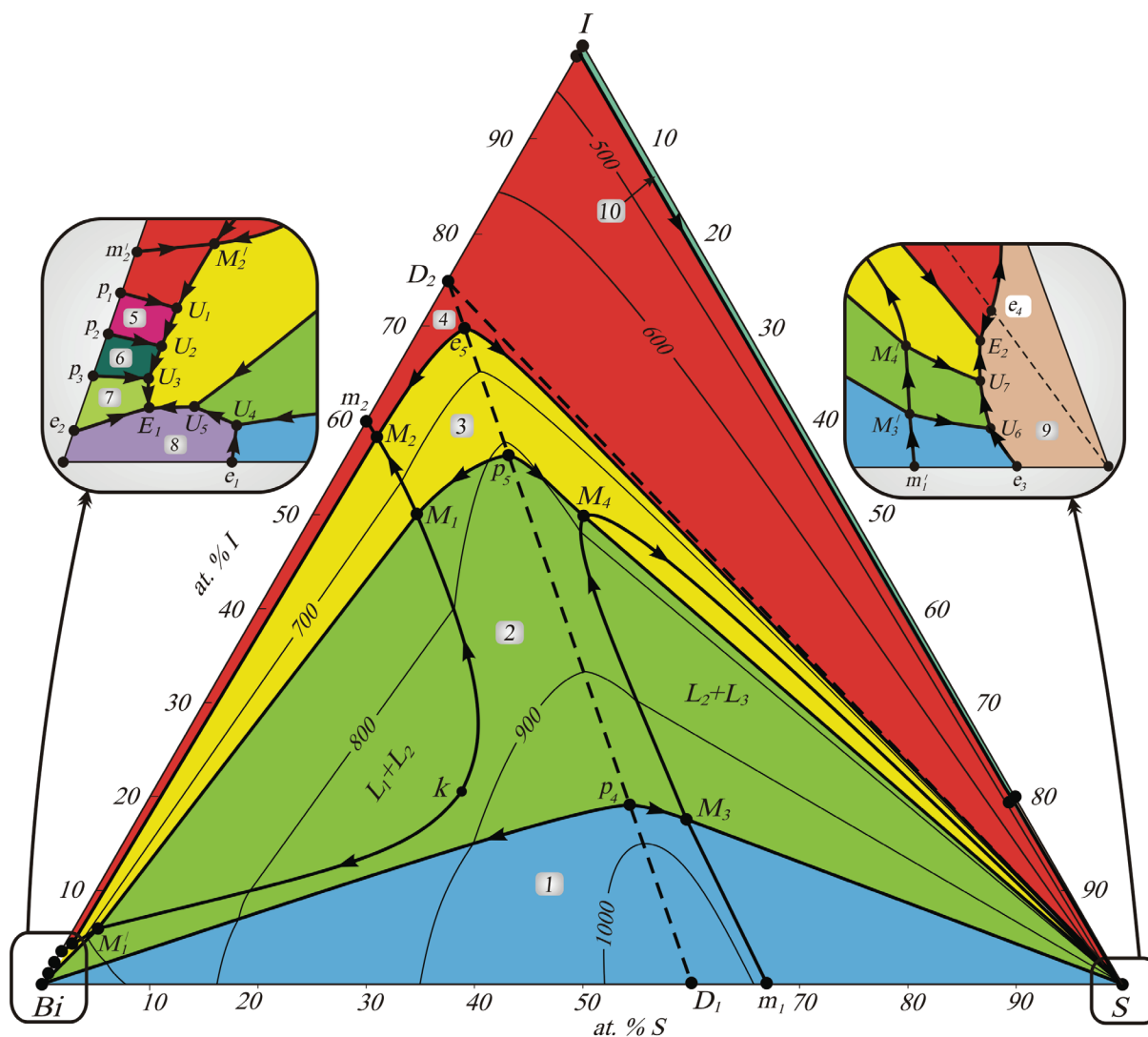


Fig. 8. The phase diagram of the Bi–S–I system [42]. Primary crystallization fields: 1 -  $\text{Bi}_2\text{S}_3$ ; 2 -  $\text{BiSI}$ ; 3 -  $\text{Bi}_{19}\text{S}_{27}\text{I}_3$ ; 4 -  $\text{BiI}_3$ ; 5 -  $\text{BiI}$ ; 6 -  $\text{Bi}_7\text{I}_2$ ; 7 -  $\text{Bi}_9\text{I}_2$ ; 8 -  $\text{Bi}$ ; 9 -  $\text{S}$ ; 10 -  $\text{I}_2$

subsystem whereas the second one ( $L_2+L_3$ ) starts from the  $\text{Bi}_2\text{S}_3$ -S subsystem ( $m_1m_1'$ ) and spreads into the  $\text{Bi}_2\text{S}_3$ - $\text{BiI}_3$ -S subsystem.

### 2.5. The Bi-Se-I system

Similar to analogous ternary systems this system also investigated mostly along the  $\text{Bi}_2\text{Se}_3$ - $\text{BiI}_3$  section. Different groups of researchers have studied this system and reported either inappropriate or contradictory results. Turjanica [47] and Belotskii [48] decided that these system hosts two ternary compounds, namely  $\text{BiSeI}$  and  $\text{Bi}_{19}\text{Se}_{27}\text{I}_3$ , while Dolgikh [49, 50] refutes the existence of the latter one. According to phase diagram drawn by Turjanica [47] and Belotskii [48] the  $\text{BiSeI}$  melts congruently at 808 K whereas, the latter one forms by peritectic reaction occur at 943 K. However, Dolgikh [49, 50] shows that the only compound,  $\text{BiSeI}$  exist in the system and it melts incongruently at 805 K. The latest version of the  $\text{Bi}_2\text{Se}_3$ - $\text{BiI}_3$  phase diagram is given in the [51] (Fig. 9). One can see that, the melting temperatures for the  $\text{BiSeI}$  compound determined in [47], [49] and [51] are very close, however, they are differ just for type of formation reaction. The phase diagram represented in [51] is very rare case that shows transition from a dystectic type to a peritectic one. This type phase diagram is possible in principle and here, there is no violation of the Gibbs phase rule. However, only thorough investigations in this area can show the correct type of formation reaction of  $\text{BiSeI}$ .

The crystal structure of the  $\text{BiSI}$  studied by various authors [52, 53]. It crystallizes in the  $\text{SbSI}$  type orthorhombic lattice system with the space

group  $Pnma$  and lattice parameters  $a = 8.697(2)$ ,  $b = 4.221(1)$ ,  $c = 10.574(2)$  Å and  $z = 4$  [53]. The phase equilibria along the  $\text{BiSeI}$ - $\text{Bi}$  and  $\text{BiSeI}$ - $\text{BiI}$  systems were studied by Chervenyyuk et al. [54]. It was found that the former one belongs to simple eutectic type, while the latter one featured by eutectic and monotectic phase diagram.

### 2.6. The Bi-Te-I system

The phase diagram of the  $\text{Bi-Te-I}$  system for the entire concentration range was first investigated by us [55]. The series of isopleth sections and the liquidus surface projection were constructed. The fields of the primary crystallization, as well as the types and coordinates of non- and monovariant equilibria were determined. Prior to our experimental work on this ternary system, it was studied in a series of works [56–58]. The greatest number of results [57–58] is devoted to the study of phase equilibria in the quasi-binary system  $\text{Bi}_2\text{Te}_3$ - $\text{BiI}_3$ . The results of [57–58] are very similar and show that the phase diagram of this system relates to a dystectic type with ternary compound  $\text{BiTeI}$  with a melting temperature of  $828 \pm 5$  K (Fig. 10). Belotskiy [33, 34] determined the melting temperature of  $\text{BiTeI}$  as 743 K and some fragments of the  $\text{Bi}_2\text{Te}_3$ - $\text{BiI}_3$  phase diagram are a little bit different than those of reported in Refs. [56–58].  $\text{BiTeI}$  crystallizes in hexagonal structure of type  $\text{CdI}_2$  with space group  $P-3ml$ , the lattice parameters:  $a = 4.31$  Å,  $c = 6.83$  Å,  $z=1$ , [56] and  $a = 4.3392$  Å,  $c = 6.854$  Å,  $z=1$  [41]. Other isopleth sections  $\text{BiI}_3$ -Te and  $\text{BiTeI}$ -Te are studied by Evdokimenko [59] and reported as simple eutectic type. Savilov [60] reported at first the exis-

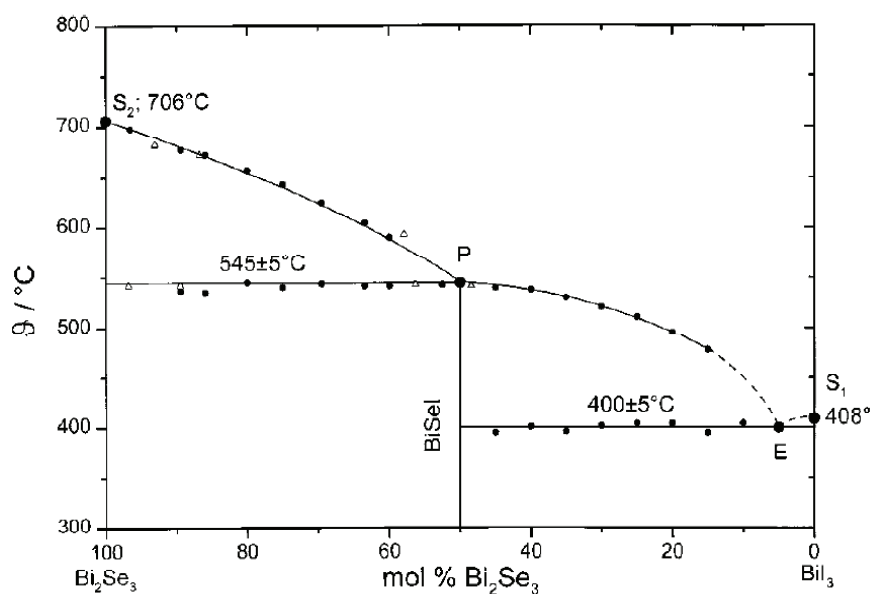
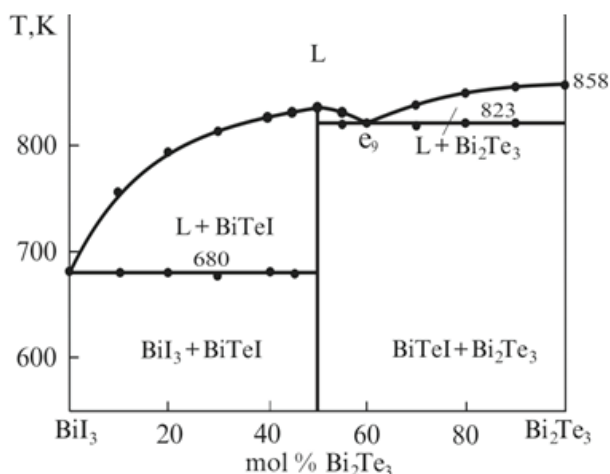


Fig. 9. Phase diagram of the quasi-binary  $\text{BiI}_3$ - $\text{Bi}_2\text{Se}_3$  system [51]



**Fig. 10.** Phase diagram of the  $\text{BiI}_3\text{-Bi}_2\text{Te}_3$  system [56-57]. Black dots shows our data [55]

tence of two new lowest telluroiodides of bismuth  $\text{Bi}_2\text{TeI}$  and  $\text{Bi}_4\text{TeI}_{1.25}$  (or  $\text{Bi}_{16}\text{Te}_4\text{I}_5$ ) obtained by condensation from the gas phase. Single crystals of the former one obtained from a melt. This compound have a monoclinic type crystal structure with lat-

tice parameters:  $a = 7.586 \text{ \AA}$ ,  $b = 4.380 \text{ \AA}$ ,  $c = 17.74 \text{ \AA}$ . The global phase diagram was constructed by us [55], where those ternary compounds were verified, their melting characters and temperatures determined. Standard thermodynamic functions of formation were also determined. The phase diagram (Fig. 11) shows the feasibility to prepare bulk single crystals of ternary compounds  $\text{BiTeI}$ ,  $\text{Bi}_2\text{TeI}$ , and  $\text{Bi}_4\text{TeI}_{1.25}$  by directional crystallization of solution melts. The quasi-binary sections divide the system  $\text{Bi-Te-I}$  on five independent subsystems:  $\text{BiI}_3\text{-TeI}_4\text{-I}$ ,  $\text{BiI}_3\text{-TeI}_4\text{-Te}$ ,  $\text{BiI}_3\text{-BiTeI-Te}$ ,  $\text{Bi}_2\text{Te}_3\text{-BiTeI-Te}$  and  $\text{Bi-Bi}_2\text{Te}_3\text{-BiI}_3$ .

### 3. CONCLUSIONS

A comparative analysis of the literature data that known so far, allows to establish that the chalcoidide systems of the antimony and bismuth exhibit very complex phase equilibrium scheme in the whole systems. They are characterized by immiscibility areas that comes from boundary binary systems. This brief review on phase diagram of these

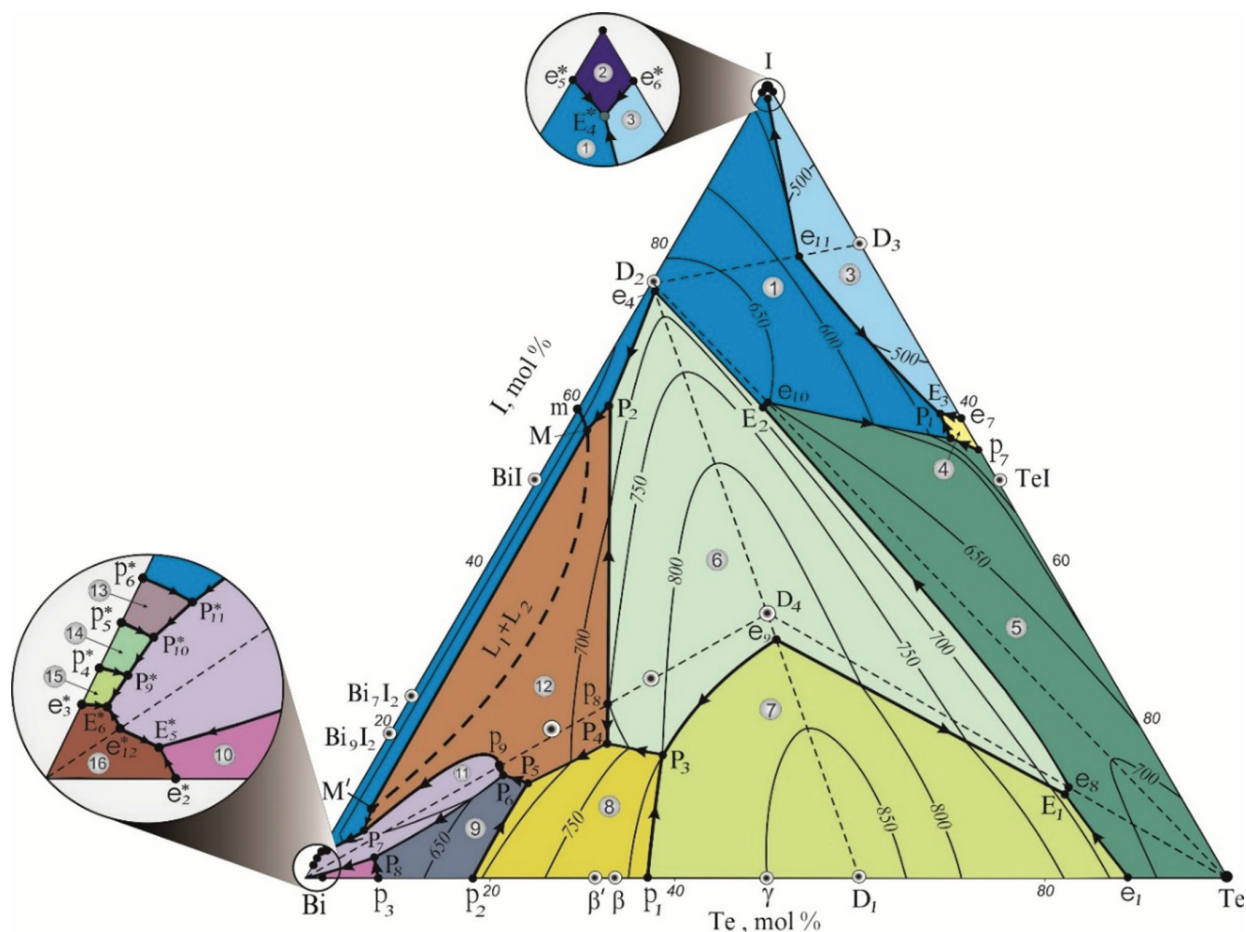


**Fig. 11.** The liquidus surface projection of the  $\text{Bi-Te-I}$  system [55]. Primary crystallization fields: 1 -  $\text{BiI}_3$ ; 2 -  $\text{I}_2$ ; 3 -  $\text{TeI}_4$ ; 4 -  $\text{TeI}$ ; 5 -  $\text{Te}$ ; 6 -  $\text{BiTeI}$ ; 7 -  $\text{Bi}_2\text{Te}_3$ ; 8 -  $\gamma$ ; 9 -  $\beta$ ; 10 -  $\beta'$ ; 11 -  $\text{Bi}_4\text{TeI}_{1.25}$ ; 12 -  $\text{Bi}_2\text{TeI}$ ; 13 -  $\text{BiI}$ ; 14 -  $\text{Bi}_7\text{I}_2$ ; 15 -  $\text{Bi}_9\text{I}_2$ ; 16 -  $\text{Bi}$



systems provides very valuable information for optimizing the synthesis and growth conditions of their known starting and intermediate ternary phases. Particularly, the considered systems are of significant importance in terms of the rational design of new multifunctional phases with variable and non-variable chemical compositions. On the other hands, information on the ternary phase diagrams of the mentioned systems are very important in growth of large single crystals from both stoichiometric and non-stoichiometric liquid phases.

### CONFLICT OF INTEREST

The author declares the absence of obvious and potential conflicts of interest related to the publication of this article.

### REFERENCES

1. Audzijonis A., Sereika R., Taltauskas R. Antiferroelectric phase transition in SbSI and SbSeI crystals. *Solid State Commun.*, 2008, v. 147(3–4), pp. 88–89. DOI: 10.1016/j.ssc.2008.05.008
2. Łukaszewicz K., Pietraszko A., Kucharska M. Diffuse Scattering, Short Range Order and Nanodomains in the Paraelectric SbSI. *Ferroelectrics*, 2008, v. 375(1), pp.170–177. DOI: 10.1080/00150190802438033
3. Audzijonis A., Gaigalas G., Tigas L., Sereika R., Taltauskas R., Balnionis D., Rēza A. Electronic structure and optical properties of BiSeI crystal. *Phys. Status Solidi B*, 2009, v. 246(7), pp. 1702–1708. DOI: 10.1002/pssb.200945110
4. Audzijonis A., Taltauskas R., Sereika R., Zigas L., Reza A. Electronic structure and optical properties of BiSI crystal. *J. Phys. Chem. Solids*. 2010, v. 71(6), pp. 884–891. DOI: 10.1016/j.jpcs.2010.03.042
5. Ganose A. M., Butler K. T., Walsh A., Scanlon D. O. Relativistic electronic structure and band alignment of BiSI and BiSeI: candidate photovoltaic materials. *J. Mater. Chem. A*, 2016, v. 4(6), pp. 2060–2068. DOI: 10.1039/c5ta09612j
6. Gerzanich E.I., Fridkin V.M. *Ferroelectric materials of type  $A^VB^VIC^VII$* . Moscow, Nauka Publ., 1982. (in Russ.)
7. Pierrefeu A., Steigmeier E. F., Dorner B. Inelastic neutron scattering in SbSI near the ferroelectric phase transformation. *Phys. Status Solidi B*, 1977, v. 80(1), pp. 167–171. DOI: 10.1002/pssb.2220800119
8. Žičkus K., Audzijonis A., Batarunas J., Šileika A. The fundamental absorption edge tail of ferroelectric SbSI. *Phys. Status Solidi B*, 1984, v. 125(2), pp. 645–651. DOI: 10.1002/pssb.2221250225
9. Rao K. K., Chaplot S. L. Dynamics of Paraelectric and Ferroelectric SbSI. *Phys. Status Solidi B*, 1985, v. 129(2), pp. 471–482. DOI: 10.1002/pssb.2221290204
10. Grigas J., Talik E., Lazauskas V. Splitting of the XPS in ferroelectric SbSI crystals. *Ferroelectrics*, 2003, v. 284(1), pp. 147–160. DOI: 10.1080/00150190390204790
11. Audzijonis A., Taltauskas R., Tigas L., Vinokurova I. V., Farberovich O. V., Pauliukas A., Kvedaravičius A. Variation of the energy gap of the SbSI crystals at ferroelectric phase transition. *Physica B*, 2006, v. 371(1), pp. 68–73. DOI: 10.1016/j.physb.2005.09.039
12. Nowak M., Nowrot A., Szperlich P., Jesionek M., Kepińska M., Starczewska A., Mistewicz K., Stróż D., Szala J., Rzychoń T., Talik E., Wrzalik R. Fabrication and characterization of SbSI gel for humidity sensors. *Sens. Actuators A*, 2014, v. 210, pp. 119–130. DOI: 10.1016/j.sna.2014.02.012
13. Ishizaka K., Bahramy M. S., Murakawa H., Sakano M., Shimojima T., Sonobe T., Koizumi K., Shin S., Miyahara H., Kimura A., Miyamoto K., Okuda T., Namatame H., Taniguchi M., Arita R., Nagaosa N., Kobayashi K., Murakami Y., Kumai R., Kaneko Y., Onose Y., Tokura Y. Giant Rashba-type spin splitting in bulk BiTeI. *Nat. Mater.*, 2011, v. 10(7), pp. 521–526. DOI: 10.1038/nmat3051
14. Landolt G., Ereemeev S. V., Koroteev Yu. M., Slomski B., Muff S., Neupert T., Kobayashi M., Strocov V. N., Schmitt T., Aliev Z. S., Babanly M. B., Amiraslanov I. R., Chulkov E. V., Osterwalder J., Dil J. H. *Phys. Rev. Lett.*, 2012, v. 109(11), p. 116403. DOI: 10.1103/physrevlett.109.116403
15. Bahramy M. S., Yang B.-J., Arita R., Nagaosa N. Emergence of non-centrosymmetric topological insulating phase in BiTeI under pressure. *Nature Commun.*, 2012, v. 3(1), p. 679. DOI: 10.1038/ncomms1679
16. Landolt G., Ereemeev S. V., Tereshchenko O. E., Muff S., Slomski B., Kokh K. A., Kobayashi M., Schmitt T., Strocov V. N., Osterwalder J., Chulkov E. V., Dil J. H. Bulk and surface Rashba splitting in single termination BiTeCl. *New J. Phys.*, 2013, v. 15(8), p. 085022. DOI: 10.1088/1367-2630/15/8/085022
17. Fiedler S., Bathon T., Ereemeev S. V., Tereshchenko O. E., Kokh K. A., Chulkov E. V., Sessi P., Bentmann H., Bode M., Reinert F. Termination-dependent surface properties in the giant-Rashba semiconductor BiTeX (X=Cl, Br, I). *Phys. Rev. B*, 2015, v. 92(23), p. 235430. DOI: 10.1103/physrevb.92.235430
18. Bahramy M. S., Ogawa N. Bulk Rashba semiconductors and related quantum phenomena. *Adv. Mater.*, 2017, v. 29(25), p. 1605911. DOI: 10.1002/adma.201605911
19. Gottstein G. *Physical Foundations of Materials Science*. Springer-Verlag Berlin Heidelberg, XIV, 2004, 502 p.
20. Babanly M. B., Chulkov E. V., Aliev Z. S., Shelvelkov A. V., Amiraslanov I. R. Phase diagrams in materials science of topological insulators based on metal chalcogenides. *Russ. J. Inorg. Chem.*, 2017, v. 62(13), pp. 1703–1729. DOI: 10.1134/s0036023617130034

21. Žičkus K., Audzijonis A., Batarunas J., Šileika A. The fundamental absorption edge tail of ferroelectric SbSI. *Phys. Status Solidi B.*, 1984, v. 125(2), pp. 645–651. DOI: 10.1002/pssb.2221250225
22. Belyayev L. M., Lyakhovitskaya V. A., Netesov G. B., Mokhosoev M.V., Aleykina S.M. Synthesis and crystallization of antimony sulfoiodide. *Izv. Akad. Nauk, Neorg. Mater.*, 1965, v. 1(12), pp. 2178–2181. (in Russ.)
23. Ryazantsev A. A., Varekha L. M., Popovkin B. A., Lyakhovitskaya V. A., Novoselova A. V.  $P$ - $T$ - $x$  phase diagram of the  $SbI_3$ - $Sb_2S_3$  system. *Izv. Akad. Nauk, Neorg. Mater.*, 1969, v. 5(7), pp. 1296–1297 (in Russ.)
24. Aliev Z. S., Musayeva S. S., Babanly M. B. The phase relationships in the Sb-S-I system and thermodynamic properties of the SbSI. *J. Phase Equilib. Diffus.*, 2017, v. 38, pp. 887–896. DOI: 10.1007/s11669-017-0601-4
25. Lukaszewicz K., Pietraszko A., Stepen' Damm Yu., Kajokas A. Crystal structure and phase transitions of the ferroelectric antimony sulfoiodide SbSI. Part II. Crystal structure of SbSI in phases I, II and III. *Pol. J. Chem.*, 1997, v. 71, pp. 1852–1857.
26. Itoh K., Matsunaga H. A study of the crystal structure in ferroelectric SbSI. *Zeitschrift für Krist.*, 1980, v. 152(3-4), p. 309–315. DOI: 10.1524/zkri.1980.152.3-4.309
27. Aliev Z. S., Musaeva S. S., Babanly D. M., Shevelkov A. V., Babanly M. B. Phase diagram of the Sb-Se-I system and thermodynamic properties of SbSeI. *J. Alloys Compd.*, 2010, v. 505(2), pp. 450–455. DOI: 10.1016/j.jallcom.2010.06.103
28. Belotskiy D. P., Lapshin V. F., Boychuk R. F., Novalkovskiy N. P. The  $Sb_2Se_3$ - $SbI_3$  system. *Izv. Akad. Nauk, Neorg. Mater.*, 1972, v. 8(3), pp. 572–574. (in Russ.)
29. Dolgikh V. A., Popovkin B. A., Odin I. N., Novoselova A. V.  $P$ - $T$ - $x$  phase diagram of the  $Sb_2Se_3$ - $SbI_3$  system. *Izv. Akad. Nauk, Neorg. Mater.*, 1973, v. 9(6), pp. 919–922. (in Russ.)
30. Rodionov Yu. I., Klokman V. V., Myakishev K. G. The solubility of semiconductor compounds  $A^{IV}B^{VI}$ ,  $A^{IV}B^{IV}$  and  $A^{VI}B^{VI}$  in halide melts. *Russ. J. Inorg. Chem.*, 1973, v. 17(3), pp. 846–849. (in Russ.)
31. Cherveniyuk G. I., Niyger F. V., Belotskiy D. P., Novalkovskiy N. P. Investigation of the phase equilibria in the SbSI-Sb, SbSI-S, SbSI-I systems. *Izv. Akad. Nauk, Neorg. Mater.*, 1977, v. 13(6), pp. 989–991. (in Russ.)
32. Aliev Z. S., Babanly M. B., Babanly D. M., Shevelkov A. V., Tedenac J. C. Phase diagram of the Sb-Te-I system and thermodynamic properties of SbTeI. *Int. J. Mat. Res.*, 2012, v. 103(3), pp. 290–295. DOI: 10.3139/146.110646
33. Belotskiy D. P., Antipov I. N., Nadtochiy V. F., Dodik S.M. Physicochemical investigations of the  $PbI_2$ - $SnI_2$ ,  $CdI_2$ - $ZnI_2$ ,  $BiI_3$ - $SbI_3$ ,  $Sb_2Te_3$ - $SbI_3$ ,  $Bi_2Te_3$ - $BiI_3$  systems. *Izv. Akad. Nauk, Neorg. Mater.*, 1969, v. 5(10), pp. 1663–1667. (in Russ.)
34. Belotskiy D. P., Dodik S. M., Antipov I. N., Nefedov Z. I. Synthesis and investigation of the telluroiodides of antimony and bismuth. *Ukr. Chem. J.*, 1970, v. 36, pp. 897–900. (in Russ.)
35. Aleshin V. A., Valitova N. R., Popovkin B. A., Novoselova A. V.  $P$ - $T$ - $x$  phase diagram of the antimony iodide system – antimony telluride. *Izv. Akad. Nauk, Zhur. Fiz. Khim.*, 1974, v. 48, p. 2395. (in Russ.)
36. Valitova N. R., Popovkin B. A., Novoselova A. V., Aslanov L. A. The compound SbTeI. *Izv. Akad. Nauk, Neorg. Mater.*, 1973, v. 9, pp. 2222–2223. (in Russ.)
37. Turyanitsa I. D., Olekseyuk I. D., Kozmanko I. I. Investigation of the  $Sb_2Te_3$ - $SbI_3$  system and properties of the compound SbTeI. *Izv. Akad. Nauk, Neorg. Mater.*, 1973, v. 9(8), pp. 433–434. (in Russ.)
38. Voutsas G. P., Rentzeperis P. J. The crystal structure of antimony selenoiodide, SbSeI. *Zeitschrift für Kristallographie*, 1983, v. 161(1–2), pp. 111–118. DOI: 10.1524/zkri.1982.161.1-2.111
39. Kikuchi A., Oka Y., Sawaguchi E. Crystal Structure Determination of SbSI. *J. Phys. Soc. Jap.*, 1967, v. 23(2), pp. 337–354. DOI: 10.1143/jpsj.23.337
40. Kichambare P., Sharon M. Preparation, characterization and physical properties of mixed  $Sb_{1-x}Bi_xTeI$ . *Solid State Ionics*, 1997, v. 101–103, pp. 155–159. DOI: 10.1016/s0167-2738(97)84024-6
41. Shevelkov A. V., Dikarev E. V., Shpanchenko R. V., Popovkin B.A. Crystal structures of bismuth tellurohalides  $BiTeX$  ( $X = Cl, Br, I$ ) from X-ray powder diffraction data. *J. Solid State Chem.*, 1995, v. 114(2), pp. 379–395. DOI: 10.1006/jssc.1995.1058
42. Aliev Z. S., Jafarov Y. I., Jafarli F. Y., Shevelkov A. V., Babanly M. B. The phase equilibria in the Bi-S-I ternary system and thermodynamic properties of the  $BiI_3$  and  $Bi_3S_2I_3$  ternary compounds. *J. Alloys Compd.* 2014, v. 610, pp. 522–528. DOI: 10.1016/j.jallcom.2014.05.015
43. Ryazantsev T. A., Varekha L. M., Popovkin B. A., Novoselova A. V.  $P$ - $T$ - $x$  phase diagram of the  $BiI_3$ - $Bi_2S_3$  system. *Izv. Akad. Nauk, Neorg. Mater.*, 1970, v. 6, pp. 1175–1179. (in Russ.)
44. Oppermann H., Petasch U. Zu den pseudobinären Zustandssystemen  $Bi_2Ch_3$ - $BiX_3$  und den ternären Phasen auf diesen Schnitten ( $Ch = S, Se, Te; X = Cl, Br, I$ ), I: Bismutsulfidhalogenide/The Pseudobinary Systems  $Bi_2Ch_3$ - $BiX_3$  and the Ternary Phases on their Boundary Lines ( $Ch = S, Se, Te; X = Cl, Br, I$ ), I: Bismuth Sulfide Halides. *Z. Naturforsch.* 2003, v. 58b, pp. 725–740. DOI: 10.1515/znb-2003-0803 (in German)
45. Haase-Wessel W. Die Kristallstruktur des Wismutsulfidjodids ( $BiSJ$ ). *Naturwissenschaften*, 1973, v. 60, pp. 474–474. DOI: 10.1007/bf00592859 (in German)
46. Miede G., Kupcik V. Die Kristallstruktur des  $Bi(Bi_2S_3)_3I_3$ . *Naturwissenschaften*, 1971, v. 58, pp. 219–219. DOI: 10.1007/bf00591851 (in German)

47. Turjanica I. D., Zajachkovskii N. F., Zajachkovskaja N. F., Kozmanko I. I. Investigation of the  $\text{BiI}_3$ - $\text{Bi}_2\text{Se}_3$  system. *Izv. Akad. Nauk, Neorg. Mater.*, 1974, v. 11(10), p. 1884. (in Russ.)
48. Belotskii D. P., Lapsin V. F., Baichuk R. F. The  $\text{BiI}_3$ - $\text{Bi}_2\text{Se}_3$  system. *Izv. Akad. Nauk Neorg. Mater.*, 1971, v. 7(11), p. 1936. (in Russ.)
49. Dolgikh V. A., Odin I. N., Popovkin B. A., Novoselova A. V.  $P$ - $T$ - $x$  phase diagram of the  $\text{BiI}_3$ - $\text{Bi}_2\text{Se}_3$  system. *Vestn. Mosk. Univ., Dep. VINITI.*, 1973, v. 23(3), Dep. No. 5683-73. (in Russ.)
50. Dolgikh V. A., Popovkin B. A., Ivanova G. I., Novoselova A. V. Investigation of the sublimation of the  $\text{SbSeI}$  and  $\text{BiSeI}$ . *Izv. Akad. Nauk, Neorg. Mater.*, 1975, v. 11(4), p. 637. (in Russ.)
51. Petasch U., Goebel H., Oppermann H. Untersuchungen zum quasibinären System  $\text{Bi}_2\text{Se}_3/\text{BiI}_3$ . *Z. Anorg. Allg. Chem.*, 1998, v. 624, p. 1767. DOI: 10.1002/(sici)1521-3749(1998110)624:11<1767::aid-zaac1767>3.0.co;2-t (in German)
52. Doenges E. Z. Über Chalkogenohalogenide des dreiwertigen Antimons und Wismuts. II. Über Selenohalogenide des dreiwertigen Antimons und Wismuts und über Antimon(III)-selenid Mit 2 Abbildungen. *Anorg. Allg. Chem.*, 1950, v. 263(5-6), pp. 280-291. DOI: 10.1002/zaac.19502630508 (in German)
53. Braun T. P., DiSalvo F. J. Bismuth selenide iodide. *Acta Crystallogr.*, 2000, v. C56(1), pp. e1-e2. DOI: 10.1107/s0108270199016017
54. Chervenyuk G. I., Babyuk P. F., Belotskii D. P., Chervenyuk T. G. Phase equilibria in the  $\text{Bi-Se-I}$  system along the  $\text{BiSeI-Bi}$  and  $\text{BiSeI-BiI}$  sections. *Izv. Akad. Nauk, Neorg. Mater.*, 1982, v. 18, pp. 1569-1572. (in Ukr.)
55. Babanly M. B., Tedenac J. C., Aliev Z. S., Balitsky D. M. Phase equilibriums and thermodynamic properties of the system  $\text{Bi-Te-I}$ . *J. Alloys Compd.*, 2009, v. 481, pp. 349-353. DOI: 10.1016/j.jallcom.2009.02.139
56. Horak J., Rodot H. Preparation de cristaux du compose  $\text{BiTeI}$ . *C. R. Acad. Sci. Paris Serie B*, 1968, v. 267(6), pp. 363-366.
57. Valitova N. R., Aleshin V. A., Popovkin B. A., Novoselova A. V. Investigation of the  $P$ - $T$ - $x$  phase diagram for the  $\text{BiI}_3$ - $\text{Bi}_2\text{Te}_3$  system. *Izv. Akad. Nauk, Neorg. Mater.*, 1976, v. 12(2), pp. 225-228. (in Russ.)
58. Tomokiyo A., Okada T., Kawanos S. Phase diagram of system  $(\text{Bi}_2\text{Te}_3)-(\text{BiI}_3)$  and crystal structure of  $\text{BiTeI}$ . *Jpn. J. Appl. Phys.* 1977, v. 16(6), pp. 291-298. DOI: 10.1143/jjap.16.291
59. Evdokimenko L. T., Tsypin M. I. The effect of halogens on the structure and properties of alloys based on  $\text{Bi}_2\text{Te}_3$ . *Izv. Akad. Nauk, Neorg. Mater.*, 1971, v. 7(8), pp. 1317-1320. (in Russ.)
60. Savilov S. V., Khrustalev V. N., Kuznetsov A. N., Popovkin B. A., Antipin Ju. M. New subvalent bismuth telluroiodides incorporating  $\text{Bi}_2$  layers: the crystal and electronic structure of  $\text{Bi}_2\text{TeI}$ . *Russ. Chem. Bull.*, 2005, v. 54(1), pp. 87-92. DOI: 10.1007/s11172-005-0221-8

УДК 546:544.016/.013:546.86/.87: 546.22/.24

DOI: 10.17308/kcmf.2019.21/1149

Поступила в редакцию 26.08.2019

Подписана в печать 15.09.2019

## ТРОЙНЫЕ СИСТЕМЫ $A^V$ - $B^{VI}$ -I: КРАТКИЙ ОБЗОР ФАЗОВЫХ РАВНОВЕСИЙ ОБЗОР

©2019 З. С. Алиев<sup>✉</sup>

*Азербайджанский государственный университет нефти и промышленности,  
Пр. Азадлыг, 20, AZ1010 Баку, Азербайджан*

**Аннотация.** В работе представлен краткий обзор по фазовым равновесиям в тройных системах  $A^V$ - $B^{VI}$ -I ( $A^V = \text{Sb, Bi}$ ;  $B^{VI} = \text{S, Se, Te}$ ). Эти системы характеризуются образованием ряда тройных соединений, являющихся перспективными базовыми материалами для фото-, термо- и ферроэлектрических преобразователей энергии. Некоторые из них демонстрируют гигантское спиновое расщепление Рашба, в результате чего на поверхности кристалла возникает уникальная тороидальная 3D поверхность Ферми, которая приводит к необычным свойствам, открывающим возможность реализации на основе этих соединений уникальных электронных устройств. Разработка методов направленного синтеза указанных соединений и мультифункциональных материалов

✉ Алиев Зия С., e-mail: ziyasaliyev@gmail.com, ziya.aliev@asoiu.edu.az

на их основе базируется на данных по фазовым равновесиям в соответствующих системах.

**Ключевые слова:** фазовая диаграмма; фазовые равновесия; сульфид сурьмы; селенид висмута; теллурид висмута.

### КОНФЛИКТ ИНТЕРЕСОВ

Автор декларирует отсутствие явных и потенциальных конфликтов интересов, связанных с публикацией настоящей статьи.

---

*Aliiev Ziya Sakhavaddin* – PhD (Chem.), Azerbaijan State Oil and Industry University, Baku, Azerbaijan; e-mail: ziyasaliev@gmail.com; ziya.aliev@asoiu.edu.az. ORCID iD 0000-0001-5724-4637.

*Алиев Зия С.* – к. х. н., Азербайджанский государственный университет нефти и промышленности, Баку, Азербайджан; e-mail: ziyasaliev@gmail.com, ziya.aliev@asoiu.edu.az. ORCID iD 0000-0001-5724-4637.